

Properties of Small Bimetallic Ni–Cu Clusters

Pedro A. Derosa,[†] Jorge M. Seminario,^{*,†} and Perla B. Balbuena^{*,‡}

Department of Electrical Engineering, and Department of Chemical Engineering, University of South Carolina, Columbia, South Carolina 29208

Received: February 7, 2001; In Final Form: June 18, 2001

Geometric and electronic properties of planar configurations of Cu–Ni clusters containing up to five atoms are studied using density functional theory with effective core potentials, focusing on the differences between mono and bimetallic clusters. Reactivity is examined by testing hydrogen adsorption on bridge and on-top sites. It is found that geometric effects have strong effect on reactivity; however, the significant differences between the Cu and Ni atomic electronic structures are strong factors on the nucleation, stability, and adsorption properties.

Introduction

Several studies have shown that bimetallic systems have certain characteristics that make them better catalysts than pure metals.^{1–4} For this reason, bimetallic nanoclusters are used in several commercial catalytic⁵ and electrocatalytic^{6,7} processes. The enhancement of the catalytic effects in bimetallic nanoparticles is determined by several factors such as overall composition, temperature, and preparation of the catalyst.^{8–13} Changes in these macroscopic variables and processes are responsible for changes at the microscopic level. For example, the above changes affect the atomistic level on the well-known surface segregation phenomena, which in turn defines the reactivity behavior of the material.^{14–17} The active components of dispersed metal catalysts are small clusters, and therefore, the cluster properties, rather than the bulk properties, are responsible for the observed characteristics.¹⁸ Thus, theoretical and experimental studies of clusters are necessary for the prediction and, eventually, for the design of the local chemistry.

Small clusters constitute an intermediate between single atoms and condensed matter. Understanding their electronic and dynamic properties and their relationship with observed macroscopic phenomena has become one of the most active areas in cluster science. Synergic approaches of theory and experiment are leading to systematic and faster advance in the field of material science.¹⁹ Experiments have revealed the relationship between electronic and geometrical structure in clusters having a number of atoms as small as 20.²⁰ On the other hand, powerful computers and efficient algorithms have allowed computational quantum chemistry to be applied to realistic systems.^{21,22} Among the huge number of papers on clusters, impossible to cite in this focused work, tight binding,^{23,24} tight-binding Friedel model,^{23,24} and ab initio methods²⁵ were used to study transition-metal clusters of up to several tens of atoms, and a modified Hückel theory was used to study coinage-metals clusters.²⁶ In addition, a combination of several methods has been used in the study of clusters, for instance, a semiempirical potential was used in a Monte Carlo calculation to study Ni_n clusters ($n = 2–13$)²⁷ and melting properties of Ni₇ and Ni₇H,^{27,28} and tight-binding molecular-dynamics was used to study geometric effects

in Ni clusters of up to 10 atoms.²⁹ Density functional theory (DFT) was used to study clusters of hundred metal atoms with partially optimized geometries using the local density (LDA) and generalized gradient (GGA) approximations³⁰ functionals. LDA was also applied to metal oxide clusters,³¹ and the Hartree–Fock method was used to study a 135 atoms cluster of metallic Be.³² Several symmetry restrictions and constraints are needed in order to have practical ab initio calculations of large clusters; the results, nevertheless, yield valuable information for the understanding of cluster behavior and its evolution to bulk. Recent studies regarding the physical properties of transition-metal clusters can be found in a recent review.³³ Interactions of clusters with small molecules were also recently reviewed.³⁴

We focus in this paper on small Cu–Ni clusters of up to five atoms in order to understand their electronic and geometric characteristics as a function of their stoichiometry. We also calculate the adsorption of H on each of the mono- and bimetallic clusters to have a preliminary assessment of their reactivity.

Procedure

DFT is nowadays one of the best methods to study small and medium-size systems;³⁵ it yields results comparable to those obtained with standard correlated ab initio methods at a computational cost similar to the lowest level, Hartree–Fock, for which the important electron correlation contribution is absent.

We have used DFT techniques^{21,22,36–40}, combined with effective core potentials (ECP)⁴¹ to optimize the geometry of several planar configurations of Cu_mNi_n ($n + m = 1–5$) clusters. Several planar structures were used as starting geometry for optimization, and those with the lowest energy were chosen. Although the planar configurations may not correspond to a cluster global minimum, they are useful for understanding the energetics and reactivity properties of bimetallic *active sites*, allowing us to compare them to active sites of similar geometry but composed of a single species. These sites may be part of bimetallic nanocatalysts where adsorption and reaction take place. As a probe system, we have investigated H adsorption on the metallic clusters. Over 200 systems were fully optimized within their corresponding point group. We used the B3PW91^{42–45}

* To whom correspondence should be addressed.

[†] Department of Electrical Engineering, University of South Carolina.

[‡] Department of Chemical Engineering, University of South Carolina.

TABLE 1: Total Population of s, p, and d Character, Spin State, and Character of the HOMO and LUMO of Ni and Ni⁺ (in Parentheses) Predicted by a Mulliken Population Analysis at the MP2, HF, and B3PW91 Levels Using LANL2DZ and 6-311G Basis Set**

	MP2 and HF ^a		B3PW91	
	LANL2DZ	6-311G**	LANL2DZ	6-311G**
s	3 (2)	7 (6)	3 (2)	8 (6)
p	6 (6)	12 (12)	6 (6)	12 (12)
d	9 (9)	9 (9)	9 (9)	8 (9)
HOMO/LUMO	α/β (β/α)	α/β (β/α)	β/β (β/α)	β/β (β/α)
α -HOMO/ α -LUMO	s/s (d/s)	s/s (d/s)	s/p (d/s)	s/s (d/s)
β -HOMO/ β -LUMO	d/s (d/s)	d/s (d/s)	d/s (d/s)	s/d (d/s)

^a Results obtained using MP2 and HF methods are identical.

functional with the Los Alamos National Laboratory (LANL2DZ) ECP which includes a double- ζ type.^{46–48} All calculations were performed using the Gaussian 94 program⁴⁹

Results and Discussion

We use all Gaussian 94 default thresholds, with the exception that the default SCF convergence of 10^{-8} could not be used for triplet of Ni₂, which converged to 10^{-6} , and for the quintet of Ni atom, which could not converge except to a useless 10^{-5} tolerance; fortunately, this quintet state does not correspond to a minimum energy electronic configuration. The quartet of Cu₂⁺¹ could not be optimized; it tends to dissociate, suggesting that it is not stable.

Cu and Ni Monomers. The Cu 3d shell is totally filled, whereas the Ni 3d is partially filled yielding compounds with strong magnetic character. Ni atom states of different multiplicity are closer in energy among each other than states of different multiplicity of Cu due to the open shell character of the Ni 3d. The fact that this d shell is filled in Cu makes it more inert than Ni and energetically well separated from the 4s shell. From a Mulliken population analysis of valence orbitals at the B3PW91/LANL2DZ, the Cu and Ni electronic configurations are $3s^23p^63d^{10}4s^1$ and $3s^23p^63d^94s^1$, respectively. Experimental and theoretical work has found that the Ni $3s^23p^63d^94s^1$ and $3s^23p^63d^84s^2$ electronic configurations are almost degenerate (within 0.03 eV).^{50,51}

The ground states of pure Cu clusters have the lowest possible multiplicity that can be obtained for a given number of unpaired electrons, whereas Ni clusters tend to have the highest.⁵⁰ The ground state of the Cu atom is a doublet, and its excited quartet is 5.8 eV above. The ground state of Ni is a triplet, and its excited singlet and quintet have energies of 1.6 and 4 eV above the triplet, respectively.

The highest occupied orbital for Cu has s character and is at 1.4 eV above the next occupied orbital, which has d character. However, the highest occupied orbital of Ni has d character. The next occupied orbital of Ni is just 0.23 eV below the highest and has s character. When Ni is ionized to Ni⁺, its electronic configuration becomes $3s^23p^63d^9$, suggesting that the s and d orbitals exchange positions, leaving the highest occupied orbital with d character. Further calculations were performed using MP2, HF, and B3PW91 (Table 1) with both LANL2DZ and 6-311G**. MP2 and HF results are practically identical. Table 1 shows the population of s, p, and d orbitals, the spin (α or β) of the highest occupied and lowest unoccupied atomic orbitals of the atoms, and the character (s, p, or d) of each spin state. Results for the cations are shown in parentheses. B3PW91/6-311G** is the only level of theory that predicts the $3s^23p^63d^8-4s^2$ configuration for Ni (28 electrons) and correctly predicts $3s^23p^63d^9$ for the ions like the other methods. Notice that the

core of Ni in the LANL2DZ ECP involves the $1s^22s^22p^6$ structure, leaving an atom with 18 electrons.

Cu and Ni Dimers. Table 2 shows predicted geometrical and energetic values for dimer structures, where the zero-point correction has been included in the reported total energy of the clusters. To assess the accuracy of our calculations, we have compared some properties of the smallest clusters to available experimental values also shown in Table 2. The experimental dimer bond length is smaller for Ni₂ than for Cu₂, whereas the calculated values show the opposite trend. This discrepancy found in the predicted bond lengths has been reported also in previous ab initio studies⁵¹ and may be attributed to the existence of several electronic states very close to the ground state. The discrepancy for Ni₂, for instance, may be due to the experimental average of several electronic states; however, the difference in bond lengths is so small that the experimental error may overcome this difference, and no real tendency can be claimed.

The Cu–Cu and Cu–Ni bond lengths are fairly estimated, differing with the corresponding experimental values by 0.04 and 0.05 Å, respectively. The Ni–Ni distance is overestimated by 0.12 Å. However, the calculated dissociation energies follow the experimental trend, higher bond length for Ni₂ than for Cu₂ (Table 2). Cu–Cu and Ni–Ni binding energies are underestimated by 0.1 eV; therefore, dimer bond lengths and binding energies are fairly well estimated differing from the experimental values by less than 6% except for the Cu–Ni bond energy, which is underestimated by 15%. The calculated vibrational frequency for Cu₂ is 256 cm^{-1} , in reasonable agreement with experimental results of 265,⁵² 266.459,⁵³ and 266.454 cm^{-1} . The calculated vibrational frequency of 280 cm^{-1} for Ni₂ is identical to that of the experimental.⁵⁵ The calculated CuNi vibrational frequency is 250 cm^{-1} , whereas the experimental is 273 cm^{-1} .^{56,57}

Table 3 shows the Mulliken population analysis of s, p, and d orbitals for two-atom clusters. A reduction in the d level population is observed in both atoms of each cluster as compared with their population in the isolated atom. This electronic redistribution opens up the 3d levels of the Cu atoms making them somewhat more similar to those of Ni atoms; however, perceptible differences are still observed in the way the presence of either Cu or Ni affects the cluster properties. The bonding population analysis (Table 3) illustrates the s character of the bond when Cu atoms are in the cluster, whereas the bond is more uniformly distributed between s, p, and d levels in Ni–Ni bond. The contributions to bonding in the CuNi cluster from the Ni atom are mostly of s character. Thus, there is an equalization effect when Cu is bonded to Ni that makes Cu to donate its s character to the bond and, therefore, yielding a weaker bond in the bimetallic cluster than in the pure metal dimer.

The ground state of Cu₂ is a singlet with the excited triplet 1.7 eV above, whereas the ground state of Ni₂ is a triplet 2.3 eV below the excited-state singlet and 4 eV below the excited quintet. The ground state of CuNi is a doublet 1.4 eV below its quartet. The 4s orbital of Cu donates charge to one of the unpaired orbitals of Ni leading to a doublet, but Ni vacates a d orbital, as a result the ground state of CuNi⁺ is a triplet.

Trimers. The optimized geometries of the trimers have C_{2v} symmetry, where the distances to the apex atom are shorter than the base length. Table 2 shows the dissociation energy of the trimer into an atom and a dimer. This energy is smaller than the dissociation energy of the dimers, and it follows an odd–even oscillatory behavior with the cluster size because of the

TABLE 2: Geometry, Multiplicity (M), Total Energy (Includes the Zero-Point Vibrational Energy), Atomic Dissociation (D_0) and Atomization Energy (ΣD_0), Vertical (V) and Adiabatic (A) Ionization Potential (IP), and Mulliken Charges of Metallic Clusters (Experimental Data in Parentheses)

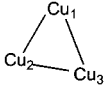
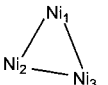
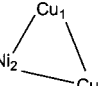
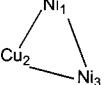
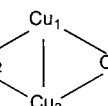
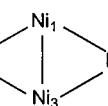
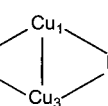
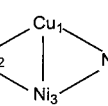
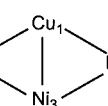
Cluster (point group)	System	M	Geometry (Å, °)	Energy (Ha)	(atom)- D_0 , (At)- ΣD_0 (eV)	IP (eV)	Charges (e)
Cu	Cu	2		-196.15426		7.69	1 = 0.0
Ni	Ni	3		-169.27959		7.60 (7.64) ^a	1 = 0.0
Cu ₂ (Dh)	Cu ₁ —Cu ₂	1	1-2 = 2.255 (2.219) ^b (2.2195) ^c (2.2197) ^d	-392.37867	1.91 (2.01) ^e (2.069) ^e	(A) 7.73 (V) 7.79	1 = 0.0 2 = 0.0
Ni ₂ (Dh)	Ni ₁ —Ni ₂	3	1-2 = 2.273 (2.155) ^f (2.1545) ^g (2.20) ^h	-338.63069	1.95 (2.042) ^g (2.068) ^h	(A) 7.47 (V) 7.75 (7.43) ^g	1 = 0.0 2 = 0.0
CuNi (Cv)	Cu ₁ —Ni ₂	2	1-2 = 2.281 (2.233) ⁱ (2.2346) ^j	-365.49951	1.79 (2.05) ^k	(A) 7.33 (V) 7.36	1 = -0.1 2 = 0.1
Cu ₃ (C _{2v})		2	1-3 = 2.686 1-2 = 2.327 2-3 = 2.327 1-2-3 = 70.5	-588.57205	(Cu)-1.06 (At)-2.97	(A) 5.64 (V) 5.77	1 = 0.0 2 = 0.1 3 = 0.0
Ni ₃ (C _{2v})		5	1-3 = 2.611 1-2 = 2.349 2-3 = 2.349 1-2-3 = 67.5	-507.95761	(Ni)-1.29 (At)-3.23	(A) 5.60 (V) 5.65	1 = 0.0 2 = 0.1 3 = 0.0
Cu ₂ Ni (C _{2v})		3	1-3 = 2.745 1-2 = 2.327 2-3 = 2.327 1-2-3 = 72.3	-561.69985	(Ni)-1.13 (Cu)-1.25 (At)-3.04	(A) 5.58 (V) 5.73	1 = -0.1 2 = 0.1 3 = -0.1
Ni ₂ Cu (C _{2v})		4	1-3 = 2.736 1-2 = 2.330 2-3 = 2.330 1-2-3 = 71.9	-534.82827	(Cu)-1.18 (Ni)-1.34 (At)-3.13	(A) 5.56 (V) 5.97	1 = -0.1 2 = 0.1 3 = -0.1
Cu ₄ (C _{2h})		1	1-2 = 2.446 1-3 = 2.302 1-4 = 2.449 2-3 = 2.449 3-4 = 2.446 2-1-4 = 123.9 2-3-4 = 123.9 1-2-3 = 56.1 1-4-3 = 56.1	-784.80717	(Cu)-2.20 (At)-5.17	(V) 6.47	1 = 0.1 2 = -0.1 3 = 0.1 4 = -0.1
Ni ₄ (C _s)		5	1-2 = 2.382 1-3 = 2.239 1-4 = 2.379 2-3 = 2.378 3-4 = 2.380 2-1-4 = 123.8 2-3-4 = 123.9 1-2-3 = 56.1 1-4-3 = 56.1	-677.31674	(Ni)-2.16 (At)-5.40	(V) 6.53	1 = 0.1 2 = -0.1 3 = 0.1 4 = -0.1
Cu ₃ Ni (C _s)		2	1-2 = 2.445 1-3 = 2.315 1-4 = 2.448 2-3 = 2.447 3-4 = 2.450 2-1-4 = 123.6 2-3-4 = 123.5 1-2-3 = 56.5 1-4-3 = 56.4	-757.93568	(Cu)-2.22 (Ni)-2.29 (At)-5.26	(V) 6.47	1 = 0.1 2 = -0.1 3 = 0.1 4 = -0.1
Cu ₂ Ni ₂ (C _s)		3	1-2 = 2.422 1-3 = 2.324 1-4 = 2.439 2-3 = 2.461 3-4 = 2.444 2-1-4 = 124.1 2-3-4 = 122.2 1-2-3 = 56.8 1-4-3 = 56.8	-731.06224	(Cu)-2.17 (Ni)-2.25 (At)-5.29	(V) 6.36	1 = 0.1 2 = -0.1 3 = 0.2 4 = -0.1
Ni ₃ Cu (C _s)		2	1-2 = 2.433 1-3 = 2.346 1-4 = 2.435 2-3 = 2.454 3-4 = 2.452 2-1-4 = 123.5 2-3-4 = 121.8 1-2-3 = 57.4 1-4-3 = 57.4	-704.19284	(Cu)-2.20 (Ni)-2.31 (At)-5.44	(V) 6.41	1 = 0.1 2 = -0.1 3 = 0.2 4 = -0.1

TABLE 2: (Continued)

Cluster (point group)	System	M	Geometry (Å, °)	Energy (Ha)	(atom)- D_o (At)- $2D_o$ (eV)	IP (eV)	Charges (e)
Cu ₅ (C _s)		2	1-3 = 2.414	-981.03080	(Cu)-1.89 (At)-7.06	(A) 5.90 (V) 6.17	1 = 0.0
			3-4 = 2.467				2 = 0.0
2-4 = 2.413	3 = 0.0						
1-5 = 2.399	4 = 0.0						
2-5 = 2.401	5 = -0.1						
3-5 = 2.448							
4-5 = 2.452							
1-3-5 = 59.1							
2-4-5 = 59.1							
Ni ₅ (C _s)		7	1-3 = 2.461				-846.67238
			3-4 = 2.437	2 = 0.0			
2-4 = 2.439	3 = 0.0						
1-5 = 2.415	4 = 0.1						
2-5 = 2.389	5 = -0.1						
3-5 = 2.459							
4-5 = 2.425							
1-3-5 = 58.8							
2-4-5 = 58.9							
Cu ₄ Ni (C _s)		3	1-2 = 2.396	-954.15448	(Cu)-1.76 (Ni)-1.84 (At)-7.02	(A) 5.71 (V) 6.01	
			2-3 = 2.439				2 = 0.0
3-4 = 2.396	3 = 0.0						
1-5 = 2.426	4 = 0.0						
2-5 = 2.489	5 = 0.0						
3-5 = 2.489							
4-5 = 2.426							
1-2-5 = 59.5							
4-3-5 = 59.5							

^a Reference 50. ^b Reference 53. ^c Reference 66. ^d Reference 50. ^e Reference 66. ^f Reference 50. ^g Reference 66. ^h Reference 50. ⁱ Reference 66. ^j Reference 50. ^k Reference 66.

TABLE 3: Population Analysis for Metallic Dimers

cluster	atom	type	total population	bonding population
Cu ₂	1 Cu	s	3.0	0.1
		p	6.1	0.0
		d	9.9	0.0
	2 Cu	s	3.0	0.1
		p	6.1	0.0
		d	9.9	0.0
Ni ₂	1 Ni	s	3.1	0.0
		p	6.1	0.0
		d	8.9	0.0
	2 Ni	s	3.1	0.0
		p	6.1	0.0
		d	8.9	0.0
CuNi	1 Cu	s	3.1	0.2
		p	6.1	0.0
		d	9.9	0.0
	2 Ni	s	2.9	0.2
		p	6.1	0.0
		d	9.0	0.0

changes in the electronic distribution caused by the addition or removal of atoms from the cluster.⁵⁸⁻⁶⁰

The atomization energy, or energy needed to dissociate the cluster into its individual atoms, is an indicator of the cluster stability. Ni₃ is the most stable and Cu₃ the lowest (Table 2). However, the highest dissociation energy for the Ni atom in the trimers is found in Ni₂Cu; i.e., it is more difficult to extract one Ni atom from Ni₂Cu than from Ni₃. The Ni-Ni bond is stronger in Ni₂Cu than in Ni₃ where the cohesive energy is more uniformly distributed among the three atoms. This effect can be observed from the relatively small energy required to extract the Cu atom in Ni₂Cu. The energy required for breaking the remaining CuNi bond after extracting one Ni from Ni₂Cu is lower than that needed to break a Ni-Ni bond after extraction of one Ni from Ni₃. The combination of these two effects gives Ni₃ higher atomization energy than Ni₂Cu but lower dissociation energy for the Ni atom than that for Ni₂Cu. A similar effect is observed for the separation of a Cu atom from Ni₂Cu and Cu₂-Ni; the dissociation energy to remove one Cu atom is slightly

higher (0.08 eV) in Cu₂Ni than in Ni₂Cu, whereas the Cu₂Ni atomization energy is slightly lower (0.09 eV) than that of Ni₂Cu.

Both pure-metal trimers show very similar electron bond population, although the bonds are stronger in the most stable cluster, Ni₃, than those in Cu₃. In the bimetallic trimers, the population is mainly of s and p character for Cu₂Ni (37% and 35% respectively) and of p and d character in CuNi₂ (44% and 42% respectively), reminiscent of atomic Ni. The apex atom (Ni in Cu₂Ni and Cu in CuNi₂) has the highest s character in both clusters because of the geometric structure rather than to the nature of the apex atom. In both cases, the apex angle is larger than each of the two vertex angles.

Cu₃ is a doublet 2.3 eV below the quartet, whereas Ni₃ is a quintet with the triplet lying only 0.06 eV above. This quasidegeneracy between spin states for Ni₃ indicates that the incomplete 3d shell is very close to the 4s level. The septet is just 0.9 eV above the quintet. The presence of Ni in the bimetallic trimers reflects in ground states with high multiplicities. For Cu₂Ni, the triplet is 0.5 eV below the singlet and 1.6 eV below the quintet, whereas for CuNi₂, the quartet is 0.5 eV below the doublet and 1.7 eV below the sextet.

Tetramers. Only planar geometries (C_s point group) of tetramers and pentamers were studied (Table 2). As expected, when the number of atoms in the cluster increases, some properties, while holding its cluster nature, show a tendency toward bulk. For instance, the average bond length for tetramers is slightly higher than for trimers, showing its tendency toward bulk values. The dissociation energy for atom extraction increases and is even higher than for the dimers, showing the odd-even oscillatory behavior typical in clusters. Like in the trimers, the bimetallic systems Cu₃Ni and Ni₃Cu have the highest dissociation energy for Cu and Ni, respectively. The atomization energy increases with the number of Ni atoms in the cluster; Ni₃Cu yields the highest atomization energy, even higher than that in the Ni tetramer. The weakest atomization energy corresponds to Cu₄.

TABLE 4: Geometry, Multiplicity (M), Total Energy (Includes the Zero-Point Vibrational Energy), Atomic Dissociation (D_0) and Atomization Energy (ΣD_0), Vertical (V) Ionization Potential (IP), and Mulliken Charges of the Hydrogenated Systems (Experimental Data in Parentheses)

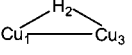
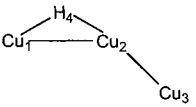
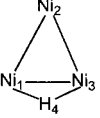
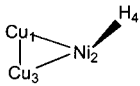
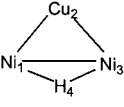
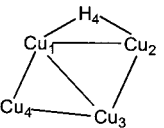
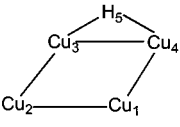
Cluster (point group)	System	M	Geometry (Å, °)	Energy (Ha)	(atom)- D_0 , (At)- ΣD_0 (eV)	IP (eV)	Charges (e)
H	H	2		-0.50101		13.63	1 = 0.0
H ₂ (D _h)	H ₁ —H ₂	1	1-2 = 0.744	-1.16388	-4.40	15.41	1 = 0.0 2 = 0.0
CuH (C _v)	Cu ₁ —H ₂	1	1-2 = 1.499	-196.77473	-2.50	9.43	1 = 0.0 2 = 0.0
NiH (C _v)	Ni ₁ —H ₂	2	1-2 = 1.485	-169.87756	-2.64	8.75	1 = 0.0 2 = 0.0
Cu ₂ H (C _s)		2	1-2 = 1.599 1-3 = 2.837 2-3 = 1.600 1-2-3 = 125.0	-392.93160	(H) -1.41 (Cu) -0.82 (At) -3.32	5.96	1 = 0.0 2 = 0.1 3 = 0.0
Ni ₂ H (C _v)	Ni ₃ —Ni ₂ —H ₁	4	1-2 = 1.541 1-3 = 3.865 2-3 = 2.324 1-2-3 = 180.0	-339.19922	(H) -1.84 (Ni) -1.14 (At) -3.78	6.17	1 = 0.0 2 = -0.1 3 = 0.1
CuNiH (C _s)	Cu ₃ —Ni ₂ —H ₁	3	1-2 = 1.536 1-3 = 3.549 2-3 = 2.340 1-2-3 = 131.4	-366.06987	(H) -1.89 (Ni) -1.17 (Cu) -1.04 (At) -3.67	6.13	1 = 0.0 2 = 0.0 3 = 0.0
Cu ₃ H (C _s)		1	1-2 = 2.411 1-3 = 4.355 2-3 = 2.284 4-1 = 1.581 4-2 = 1.764 1-2-3 = 136.1 1-4-2 = 92.1 4-1-2-3 = -179.7	-589.15797	(H) -2.31 (Cu) -1.96 (At) -5.28	6.69	1 = 0.1 2 = 0.0 3 = -0.2 4 = 0.0
Ni ₃ H (C _s)		4	1-2 = 2.422 1-3 = 2.286 2-3 = 2.422 1-4 = 1.715 3-4 = 1.715 1-2-3 = 56.3 4-2-1 = 28.2 4-3-2-1 = 1.4	-508.56603	(H) -2.92 (Ni) -2.37 (At) -6.16	6.78	1 = 0.1 2 = -0.1 3 = 0.1 4 = -0.1
Cu ₂ NiH (C _s)		2	1-2 = 2.466 1-3 = 2.311 2-3 = 2.466 4-2 = 1.578 1-2-3 = 55.9 4-2-1-3 = -128.1	-562.29471	(H) -2.55 (Cu) -1.92 (Ni) -2.27 (At) -5.59	6.74	1 = 0.1 2 = -0.1 3 = 0.1 4 = -0.1
Ni ₂ CuH (C _s)		5	1-2 = 2.413 1-3 = 2.555 2-3 = 2.413 1-4 = 1.694 3-4 = 1.694 1-2-3 = 63.9 1-4-3 = 97.9 4-1-2-3 = 0.0	-535.41009	(H) -2.20 (Ni) -1.65 (Cu) -1.54 (At) -5.32	6.05	1 = 0.0 2 = 0.0 3 = 0.0 4 = 0.0
Cu ₄ H (C ₁)		2	1-2 = 2.395 1-3 = 2.478 1-4 = 2.384 2-3 = 2.473 3-4 = 2.426 1-5 = 1.691 2-5 = 1.715 2-1-4 = 120.8 2-3-4 = 116.0 1-2-3 = 61.2 1-4-3 = 62.0 1-5-2 = 89.4	-785.39387	(H) -2.33 (Cu) -2.22 (At) -7.50		1 = 0.1 2 = -0.1 3 = 0.0 4 = -0.1 5 = 0.0
Ni ₄ H (C ₁)		6	1-2 = 2.445 1-3 = 2.540 1-4 = 2.401 2-3 = 2.370 3-4 = 2.377 3-5 = 1.695 4-5 = 1.723 2-1-4 = 114.2 2-3-4 = 118.0 1-2-3 = 63.7 1-4-3 = 64.2 3-5-4 = 88.1	-677.97577	(H) -2.67 (Ni) -1.91 (At) -8.06		1 = 0.0 2 = -0.1 3 = 0.1 4 = -0.1 5 = 0.0

TABLE 4: (Continued)

Cluster (point group)	System	M	Geometry (Å, °)	Energy (Ha)	(atom)- D_o , (At)- ΔD_o (eV)	IP (eV)	Charges (e)
Cu ₃ NiH (C ₁)		3	1-2 = 2.428	-758.52500	(H) -2.40 (Ni) -2.38 (Cu) -2.07 (At) -7.66		1 = 0.1
			1-3 = 2.458				2 = -0.1
			1-4 = 2.458				3 = 0.1
			2-3 = 2.386				4 = -0.1
			3-4 = 2.431				5 = 0.0
			3-5 = 1.695				
			4-5 = 1.723				
			2-1-4 = 117.7				
			2-3-4 = 120.5				
			1-2-3 = 61.4				
1-4-3 = 60.4							
3-5-4 = 90.7							
Ni ₂ Cu ₂ H (C ₁)		2	1-2 = 2.413	-731.65776	(H) -2.57 (Ni) -2.27 (Cu) -2.54 (At) -7.86		1 = 0.1
			1-3 = 2.405				2 = -0.1
			1-4 = 2.471				3 = 0.1
			2-3 = 2.424				4 = 0.0
			3-4 = 2.396				5 = 0.0
			3-5 = 1.683				
			4-5 = 1.738				
			2-1-4 = 119.2				
			2-3-4 = 121.9				
			1-2-3 = 59.6				
1-4-3 = 59.2							
3-5-4 = 88.9							
Ni ₃ CuH (C ₁)		3	1-2 = 2.469	-704.78655	(H) -2.52 (Ni) -1.64 (Cu) -2.80 (At) -7.96		1 = 0.0
			1-3 = 2.426				2 = 0.0
			1-4 = 2.418				3 = 0.1
			2-3 = 2.389				4 = -0.1
			3-4 = 2.419				5 = 0.0
			2-5 = 1.734				
			3-5 = 1.688				
			2-1-4 = 118.3				
			2-3-4 = 121.6				
			1-2-3 = 59.9				
1-4-3 = 60.2							
2-5-3 = 88.5							
Cu ₅ H (C ₁)		1	1-2 = 2.409	-981.62641	(H) -2.57 (Cu) -2.13 (At) -9.63	6.63	1 = 0.1
			2-3 = 2.456				2 = 0.0
			3-4 = 2.448				3 = 0.0
			1-5 = 2.408				4 = 0.0
			2-5 = 2.365				5 = -0.1
			3-5 = 2.718				6 = 0.0
			4-5 = 2.330				
			4-6 = 1.725				
			5-6 = 1.687				
			1-2-5 = 60.6				
4-3-5 = 53.3							
4-6-5 = 86.1							
6-5-2-3 = 0.3							
Ni ₅ H (C ₁)		6	1-3 = 2.414	-847.27574	(H) -2.78 (Ni) -2.19 (At) -10.25	6.29	1 = 0.0
			3-4 = 2.445				2 = 0.0
			4-2 = 2.381				3 = -0.1
			1-5 = 2.352				4 = 0.1
			2-5 = 2.426				5 = 0.0
			3-5 = 2.586				6 = 0.0
			4-5 = 2.396				
			1-6 = 1.697				
			5-6 = 1.683				
			1-3-5 = 56.0				
2-4-5 = 61.0							
1-6-5 = 88.2							
6-5-4-2 = -141.3							
Cu ₄ NiH (C ₁)		2	1-2 = 2.440	-954.76074	(H) -2.86 (Ni) -2.37 (Cu) -2.22 (At) -9.88	6.49	1 = 0.1
			2-3 = 2.489				2 = 0.0
			3-4 = 2.481				3 = 0.0
			1-5 = 2.399				4 = 0.1
			2-5 = 2.369				5 = -0.2
			3-5 = 2.562				6 = 0.0
			4-5 = 2.329				
			4-6 = 1.782				
			5-6 = 1.665				
			1-2-5 = 59.8				
4-3-5 = 55.0							
4-6-5 = 85.0							
6-5-2-3 = -1.7							

The presence of Ni atoms tends to increase the cluster multiplicity with the exception of CuNi₃, which is a doublet; thus, the planar structure is not the global minimum for this cluster, and we expect that a three-dimensional structure yields a lower energy resulting in a higher multiplicity configuration.

Pentamers. Like in the tetramers, we found a small increase in the average bond length in these clusters with respect to the smaller systems studied in this work. The dissociation energy for each atom is lower for these clusters than for tetramers, following the odd-even oscillation pattern. On the other hand,

the Cu and Ni dissociation energies in Cu₄Ni are lower than those in Cu₅ and Ni₅, respectively. This difference with most of the systems discussed in previous sections may be attributed to a geometric effect. In pure-metal pentamers, the angle between the three atoms located in the base of the cluster is 179.8°, whereas in Cu₄Ni, it is 175.4°, because the inserted Ni atom moved outward from the center of the structures. For this reason, the bond length of Ni to each of the Cu atoms increases in the bimetallic cluster and the corresponding bond becomes weaker.

A population analysis of the Ni₅ cluster reveals that atoms 1 and 2 (Table 2) have higher *s* population than those of the corresponding atoms in Cu₅, whereas the rest of the atoms have *s* populations lower than those in Cu₅. As the cluster size increases, *p* levels become more populated. Increments of up to 0.82 electrons are observed for the five-atom clusters, corresponding to the central atom in the monometallic clusters; this indicates that 4*p* have hybridized with *s* and *d* orbitals. The Cu₅ molecular orbitals (MOs) are made of 16% *s*, 35% *p*, and 49% *d* character; however, the Ni₅ MOs are 15% *s*, 33% *p*, and 52% *d* character. On the other hand, the atomic contributions for Cu₄Ni, 15% *s*, 34% *p*, and 51% *d*, seem to be an average of the corresponding contributions for Cu₅ and Ni₅.

The oscillation in the dissociation energy of one Ni atom with respect to the number of atoms in monometallic clusters is less pronounced than the oscillation observed when one Cu atom is extracted from a Cu cluster most likely because of a competition between *ionization* from *sp* levels and *d* levels.⁶⁰ In the case of bimetallics, the same effect is observed when comparing clusters containing one Ni atom and a variable number of Cu atoms with those having one Cu atom and a variable number of Ni atoms. The energy needed to extract one atom (of either Cu or Ni) is higher for clusters with even number of atoms. Atomization energies per atom yield the same oscillatory behavior as the number of atoms in the cluster varies.

The average work function for Ni is 5.15 eV, and for Cu, it is 4.65 eV.⁶¹ Calculated ionization (IP) potentials for Cu clusters are higher than those of their corresponding monomer, dimer, and trimer Ni clusters. For tetramers and pentamers, this trend reverts, and the IP approaches the bulk metal value. The overall tendency of the IP for pure metal cluster is to decrease toward bulk values. The bimetallic clusters show lower IP than pure-metal clusters. A higher IP is observed for Cu₂Ni than for Ni₂-Cu. Accordingly, Cu₃Ni has the highest IP for the bimetallic tetramers followed by Ni₃Cu; however, the values reported in Table 2 for the tetramer are the vertical IP, and the tendency could be different than for the adiabatic IP. In the case of the pentamer, the IP for Cu₅ is 0.19 eV larger than that for Cu₄Ni. Higher IP implies higher electronic stability against electron ejection. The lowest bond stability of Cu clusters could be then attributed to the nature of the orbitals; the lowest binding energy indicates a less bonding character of the orbitals in Cu than in Ni which is manifested by the lower bond population observed in Cu.

Hydrogen Adsorption. Table 4 shows the geometric and energetic properties of the metallic clusters with one adsorbed H atom. In all cases, the H–Ni bond is stronger than the H–Cu bond. The energy required for desorption of the H atom from bimetallic clusters is higher than that needed for desorption of H from pure Cu clusters of the same number of atoms. Among the investigated clusters, we found only two cases whereby the H binding energy to H–Ni_{*x*}Cu_{*y*} bimetallic clusters was higher than that of a H–Ni_{*n*} cluster with *n* = *x* + *y*; the two cases correspond to *x* = 1 with *y* = 1 and *x* = 1 with *y* = 4. H atoms

TABLE 5: Bond Energies and Lengths of CuH and NiH Using the B3PW91 Functional with LANL2DZ and 6-311G Basis Set Compared with Experimental Results**

	LANL2DZ		6-311G**		experiment	
	bond energy	bond length	bond energy	bond length	bond energy	bond length
CuH	2.61	1.499	3.30	1.435	2.75 ^a	1.46257 ^b
NiH	2.75	1.485	1.61	1.499	2.70 ^c	1.46 ^c , 1.454 ^d

^a Reference 51. ^b Reference 62. ^c Reference 6. ^d Reference 64.

prefer to migrate bonding to Ni atoms, even when the H atom is not initially bonded to Ni atoms during the geometry optimization. Several top and bridge sites were tested yielding several local minima as well as transition states, which were further investigated to find their corresponding local minima. We report in Table 4 the lowest energy case from each of the systems.

Table 5 shows the experimental bond length and binding energy, for CuH it is 1.463 Å⁶² and 2.75 eV,⁵¹ respectively, and the corresponding values for NiH are 1.46 Å⁶³ and 1.454 Å⁶⁴ and 2.70 eV,⁵¹ respectively. Because of the small disagreement between these theoretical results and the experimental ones, we checked if the use of a full electron basis set could improve the results of the effective core potential. We used the 6-311G** basis set for NiH and CuH to calculate dissociation energies and bond lengths. The full basis set practically converged to an excited state rather than the ground state, as can be noticed in Table 5, suggesting that ECP calculations are more practical than full electron calculations.

The calculated vibrational frequency for CuH dimer is 1839 cm⁻¹, and the experimental value is 1940.75 cm⁻¹.⁶² For NiH, the calculated value is 1871 cm⁻¹ and the experimental value is 2001.3 cm⁻¹.⁶⁴ The calculated dipole moment for NiH is 2.74 D, whereas the experimental is 2.4 D.⁶⁵ The calculated dipole moment of CuH is 2.97 D, but no experimental result is available. Previous *ab initio* results using an expensive multi-configurational second-order perturbation theory yielded 2.342 D for NiH, in better agreement with the experiment, and 2.66 D for CuH.⁵¹

Some of the other configurations found to be local minima for Cu₂H and Ni₂H are almost degenerate with those shown in Table 4. For Cu₂H, the ground-state energy for the linear cluster HCu₂ is only 0.15 eV above the bent configuration. The linear NiHNi is 0.2 eV above HNiNi, and the linear configuration CuNiH is a transition state, 0.03 eV above the minimum shown in Table 4.

The energy required to extract a metal atom from a hydrogenated cluster oscillates with the number of atoms in the cluster. The H–Cu bond length was found between 1.5 and 1.6 Å for on-top adsorption and between 1.58 and 1.69 Å for adsorption on a bridge site. The H–Ni bond length varies between 1.48 and 1.58 Å for on-top adsorption, whereas it is between 1.66 and 1.71 Å for adsorption on a bridge site. When H is adsorbed on a top site, the metal–metal bond length from the metal atom attached to H is longer (weaker) than in the bare cluster, whereas metal–metal bonds, for metal atoms not directly in contact with H, are shorter (stronger). On the other hand, for H adsorption on a bridge site, the metal–metal bond length of the two atoms bonded to H is shorter (stronger) than in the bare cluster, except for the pure-Cu trimer. The metal–metal bond length between atoms that are not nearest neighbors to H depends, instead, on geometric and electronic factors.

Clusters of odd number of atoms decrease their multiplicity in one when attached to an H because the electron from H pairs

one of the metal unpaired electrons with the sole exception of Ni_2Cu that is a quartet and becomes a quintet; however, the triplet is only 0.4 eV above. On the other hand, multiplicity of clusters with even number of atoms increases when attached to an H because the addition of a new unpaired electron to the system with the exception of ground-state triplet Cu_2Ni_2 , which becomes a doublet when H is adsorbed yet at only 0.07 eV below the quartet.

The differences in the electronic structures of Cu and Ni reflect in their interaction with H. Several states are very close in energy, and minor changes in the geometry could modify the ground-state multiplicity. For example, the octet and quartet of Ni_5H are just 0.3 and 0.08 eV, respectively, above the ground-state sextet.

Geometric effects determine the charge distribution as shown in Table 2. Negative charge tends to concentrate in less coordinated atoms of trimers and tetramers and in atoms with higher coordination number in compacted structures, such as planar pentamers. Ni donates charge in CuNi and NiH . When H is adsorbed (Table 4) and its closest neighbor is Ni, H always becomes slightly negative. If H is adsorbed "on top" position (HNiNi , HNiCu , and HNiCu_2) both H and Ni accept electrons from the other atoms in the cluster. Also, if H is adsorbed on a "bridge" position like in HNi_3 , HNi_2Cu , and all four-atom systems, the charge on H is always negative except in the pure Cu clusters. The charge of the bridge atoms depends on the cluster geometry, and like in the bare clusters, the atoms with the highest bond length in the cluster are negatively charged. Cu donates charge to H in CuH but not in dimers and trimers having two Cu as nearest neighbors to H where the charge on the H atom is positive.

Conclusions

Differences in physical and reactivity properties of the clusters can be tracked down to the atomic structure as well as to geometric factors. Pure Ni clusters have higher atomization energy than Cu or Cu–Ni clusters, whereas no clear trend is found comparing Cu and Cu–Ni clusters. The dissociation energy oscillates as the number of atoms in the cluster changes from odd to even, with those with an even number of atoms showing better stabilities.

Ni clusters yield stronger binding than Cu clusters to adsorb H, and for dimers and pentamers, bimetallic clusters yield the highest binding to H. These preliminary results indicate that Cu clusters with small concentrations of Ni could be the best adsorbents for H. The preferred adsorption site is close to Ni. When adsorbed on bridge sites, H tends to strengthen the metal–metal bond of nearby metallic atoms, whereas if it is adsorbed on top sites, the nearest metal–metal bond becomes weakened.

Acknowledgment. J.M.S. appreciates the support of DARPA/ONR under Grants N00014-99-1-0406 and N00000-01-1-0000 and ARO under Grants DAAD19-00-1-0154 and DAAD19-99-1-0085. P.B.B. gratefully acknowledges financial support from NSF CAREER award Grant CTS-9876065 and ARO Grant DAAD19-00-1-0087. Computer resources from NCSA, NERSC, and NASA are also acknowledged.

References and Notes

- Sinfelt, J. H. Bifunctional Catalysis. *Adv. Chem. Eng.* **1964**, *5*, 37.
- Sinfelt, J. H. Catalysis by Alloys and Bimetallic Catalysts. *Acc. Chem. Res.* **1977**, *10*, 15.
- Sinfelt, J. H. *Bimetallic Catalysts. Discoveries, Concepts and Applications*; Wiley: New York, 1983.
- Bazin, D.; Mottet, C.; Treglia, G. New opportunities to understand heterogeneous catalysis processes on nanoscale bimetallic particles through synchrotron radiation and theoretical studies. *Appl. Catal. A: General* **2000**, *200*, 47–54.
- Toshima, N.; Yonezawa, T. Bimetallic nanoparticles—novel materials for chemical and physical applications. *New J. Chem.* **1998**, *22*, 1179–1201.
- Tess, M. E.; Hill, P. L.; Torraca, K. E.; Kerr, M. E.; Abboud, K. A.; McElwee-White, L. Bimetallic Pt/Ru complexes as catalysts for the electrooxidation of methanol. *Inorg. Chem.* **2000**, *39*, 3942–3944.
- Bonnemann, H.; Brinkmann, R.; Britz, P.; Endruschat, U.; Mortel, R.; Paulus, U. A.; Feldmeyer, G. J.; Schmidt, T. J.; Gasteiger, H. A.; Behm, R. J. Nanoscopic Pt-bimetal colloids as precursors for PEM fuel cell catalysts. *J. New Mater. Electrochem. Syst.* **2000**, *3*, 199–206.
- Goodman, D. W.; Peden, C. H. F. Hydrogen Spillover from Ruthenium to Copper in Cu/Ru catalysts: a potential source of error in active metal titration. *J. Catal.* **1985**, *95*, 321.
- Goodman, D. W. Surface properties of mixed-metal catalysts, *ACS Symp. Ser.* **1989**, *411*, 191.
- Hills, C. W.; Nashner, M. S.; Frenkel, A. I.; Shapley, J. R.; Nuzzo, R. G. Carbon Support Effects on Bimetallic Pt–Ru Nanoparticles Formed from Molecular Precursors. *Langmuir* **1999**, *15*, 690–700.
- Nashner, M. S.; Frenkel, A. I.; Adler, D. L.; Shapley, J. R.; Nuzzo, R. G. Structural characterization of carbon-supported platinum–ruthenium nanoparticles from the molecular cluster precursor $\text{PtRu}_5\text{C}(\text{CO})_{16}$. *J. Am. Chem. Soc.* **1997**, *119*, 7760.
- Nashner, M. S.; Frenkel, A. I.; Somerville, D.; Hills, C. W.; Shapley, J. R.; Nuzzo, R. G. Core Shell Inversion during Nucleation and Growth of Bimetallic Pt/Ru Nanoparticles. *J. Am. Chem. Soc.* **1998**, *120*, 8093–8101.
- Pan, C.; Dassenoy, F.; Casanove, M. J.; Philippot, K.; Amiens, C.; Lecante, P.; Mosset, A.; Chaudret, B. A New Synthetic Method toward Bimetallic Ruthenium Platinum Nanoparticles; Composition Induced Structural Changes. *J. Phys. Chem. B* **1999**, *103*, 10098–10101.
- Adams, R. D. Metal segregation in bimetallic clusters and its possible role in synergism and bifunctional catalysis. *J. Organomet. Chem.* **2000**, *600*, 1–6.
- Mainardi, D. S.; Balbuena, P. B. Monte Carlo simulation studies of surface segregation in copper–nickel nanoclusters. *Langmuir* **2001**, *17*, 2047–2050.
- VanderWiel, D. P.; Pruski, M.; King, T. S. A kinetic study on the adsorption and reaction of hydrogen over silica-supported ruthenium and silver–ruthenium catalysts during the hydrogenation of carbon monoxide. *J. Catal.* **1999**, *188*, 186–202.
- Howe, J. M. *Interfaces in Materials*; John Wiley & Sons: New York, 1997.
- Knickelbein, M. B. Reactions of transition metal clusters with small molecules. *Annu. Rev. Phys. Chem.* **1999**, *115*, 50–79.
- Pauwels, B.; VanTendeloo, G.; Bouwen, W.; Kuhn, L. T.; Lievens, P.; Lei, H.; Hou, M. Low-energy deposited Au clusters investigated by high-resolution electron microscopy and molecular dynamics simulations. *Phys. Rev. B* **2000**, *62*, 10383–10393.
- Winter, B. J.; Parks, E. K.; Riley, S. J. Copper Clusters – The Interplay Between Electronic and Geometrical Structure. *J. Chem. Phys.* **1991**, *94*, 8618–8621.
- Seminario, J. M., Ed.; *Recent Developments and Applications of Modern Density Functional Theory*; Elsevier Science Publishers: Amsterdam, 1996.
- Chong, D. P., Ed.; *Recent Advances in Density Functional Theory (Part I)*; World Scientific: Singapore, 1995.
- Zhao, J. J.; Han, M.; Wang, G. H. Ionization potentials of transition-metal clusters. *Phys. Rev. B* **1993**, *48*, 15297–15300.
- Zhao, J.; Chen, X.; Wang, G. Critical Size for a Metal–Nonmetal Transition in Transition–Metal Clusters. *Phys. Rev. B* **1994**, *50*, 15424–15426.
- Demuyneck, J.; Rohmer, M.-M.; Strich, A.; Veillard, A. Bulk Properties or not: The Electronic Structure of Small Metal Clusters. *J. Chem. Phys.* **1981**, *75*, 3443–3453.
- Zhao, J.; Chen, X.; Wang, G. Structure and Ionization Potential of Coinage-Metal Clusters. *Phys. Lett. A* **1994**, *189*, 223–226.
- Curotto, E.; Matro, A.; Freeman, D. L. A Semiempirical Potential for Simulations of Transition Metal Clusters: Minima and Isomers of Ni_n ($n = 2–13$) and their Hydrides. *J. Chem. Phys.* **1998**, *108*, 729–742.
- Curotto, E.; Freeman, D. L.; Chen, B.; Doll, J. D. The Melting Transition of Ni_7 and Ni_7H as Modeled by a Semiempirical Potential. *Chem. Phys. Lett.* **1998**, *295*, 366–372.
- Menon, M.; Connolly, J.; Lathiotakis, N.; Andriotis, A. Tight-Binding Molecular-Dynamics Study of Transition–Metal Clusters. *Phys. Rev. B* **1994**, *50*, 8903–8906.
- Häberlen, O. D.; Chung, S.-C.; Stener, M.; Rösch, N. From Cluster to bulk: A Relativistic Density Functional Investigation on a Series of Gold Cluster Aun, $n = 6, \dots, 147$. *J. Chem. Phys.* **1997**, *106*, 5189–5201.

- (31) Pacchioni, G.; Chung, S. C.; Kruger, S.; Rösch, N. On the evolution of cluster to bulk properties: a theoretical LCGTO-LDF study of free and coordinated Nin clusters ($n = 6-147$). *Chem. Phys.* **1994**, *184*, 125–137.
- (32) Ross, R. B.; Ermiler, W. C.; Kern, C. W.; Pitzer, R. M. Ab initio studies of the electronic structure and density of states of metallic beryllium. *Int. J. Quantum Chem.* **1992**, *41*, 733–747.
- (33) Alonso, J. A. Electronic and Atomic Structure, and Magnetism of Transition-Metal Clusters. *Chem. Rev.* **2000**, *100*, 637–677.
- (34) Knichelbein, M. B. Reactions of Transition Metal Clusters with Small Molecules. *Annu. Rev. Phys. Chem.* **1999**, *50*, 79–115.
- (35) Foresman, J. B.; Frisch, A. *Exploring chemistry with electronic structure methods*; Gaussian, Inc.: Pittsburgh, PA, 1996.
- (36) Seminario, J. M.; Politzer, P., Eds.; *Modern Density Functional Theory: A Tool for Chemistry*; Elsevier: Amsterdam, 1995.
- (37) Parr, R. G.; Yang, W. *Density Functional Theory of Atoms and Molecules*; Oxford University Press: Oxford, U.K., 1989.
- (38) Kryachko, E. S.; Ludeña, E. *Energy Density Functional Theory of Many-Electron Systems*; Academic Press: New York, 1990.
- (39) Dreizler, R. M.; Gross, E. K. U. *Density Functional Theory*; Springer-Verlag: Berlin, 1990.
- (40) Labanowski, J. K.; Andzelm, J. W. *Density functional methods in chemistry*; Springer-Verlag: New York, 1991.
- (41) Dunning, T. H.; Hay, P. J. Gaussian Basis Sets for Molecular Calculations. In *Methods of Electronic Structure Theory*; Schaefer, H. F., III, Ed.; Plenum: New York, 1976; pp 1–28.
- (42) Becke, A. D. Density-functional thermochemistry. III. The role of exact exchange. *J. Chem. Phys.* **1993**, *98*, 5648–5652.
- (43) Perdew, J. P. Unified theory of exchange and correlation beyond the local density approximation. In *Electronic Structure of Solids*; Ziesche, P., Eschrig, H., Eds.; Akademie Verlag: Berlin, 1991.
- (44) Perdew, J. P.; Chevary, J. A.; Vosko, S. H.; Jackson, K. A.; Pederson, M. R.; Singh, D. J.; Fiolhais, C. Atoms, molecules, solids and surfaces: applications of the generalized gradient approximation for exchange and correlation. *Phys. Rev. B* **1992**, *46*, 6671–6687.
- (45) Perdew, J. P.; Wang, Y. Accurate and simple analytic representation of the electron-gas correlation energy. *Phys. Rev. B* **1992**, *45*, 13244–13249.
- (46) Hay, P. J.; Wadt, W. R. Ab initio effective core potentials for molecular calculations. Potentials for the transition metal atoms Sc to Hg. *J. Chem. Phys.* **1985**, *82*, 270–283.
- (47) Wadt, W. R.; Hay, P. J. Ab initio effective core potentials for molecular calculations. Potentials for main group elements Na to Bi. *J. Chem. Phys.* **1985**, *82*, 284–298.
- (48) Hay, P. J.; Wadt, W. R. Ab initio effective core potentials for molecular calculations. Potentials for K to Au including the outermost core orbitals. *J. Chem. Phys.* **1985**, *82*, 299–310.
- (49) Frisch, M. J.; Trucks, G. W.; Schlegel, H. B.; Gill, P. M. W.; Johnson, B. G.; Robb, M. A.; Cheeseman, J. R.; Keith, T.; Petersson, G. A.; Montgomery, J. A.; Raghavachari, K.; Al-Laham, M. A.; Zakrzewski, V. G.; Ortiz, J. V.; Foresman, J. B.; Cioslowski, J.; Stefanov, B. B.; Nanayakkara, A.; Challacombe, M.; Peng, C. Y.; Ayala, P. Y.; Chen, W.; Wong, M. W.; Andres, J. L.; Replogle, E. S.; Gomperts, R.; Martin, R. L.; Fox, D. J.; Binkley, J. S.; Defrees, D. J.; Baker, J.; Stewart, J. P.; Head-Gordon, M.; Gonzalez, C.; Pople, J. A. *Gaussian 94*; Gaussian, Inc.: Pittsburgh, PA, 1995.
- (50) Reuse, F. A.; Khanna, S. N. Geometry, Electronic-Structure, and Magnetism of Small Nin ($n = 2-6, 8, 13$) Clusters. *Chem. Phys. Lett.* **1995**, *234*, 77–81.
- (51) Pou-Américo, R.; Merchán, M.; Nebot-gil, I.; Malmqvist, P.-Å.; Roos, B. O. The Chemical-Bonds in CuH, Cu₂, NiH, and Ni₂ Studied with Multiconfigurational Second-Order Perturbation Theory. *J. Chem. Phys.* **1994**, *101*, 4893–4902.
- (52) Leopold, D. G.; Ho, J.; Lineberger, W. C. Photoelectron Spectroscopy of Mass-Selected Metal Cluster Anions. Cu– n , $n = 1-10$. *J. Chem. Phys.* **1987**, *86*, 1715–1726.
- (53) Ram, R. S.; Jarman, C. N.; Bernath, P. F. Fourier Transform Emission Spectroscopy of the Copper Dimer. *J. Mol. Spectrosc.* **1992**, *156*, 468–486.
- (54) Rohlfing, E. A.; Valentini, J. J. UV Laser Exited Fluorescence Spectroscopy of the Jet-Cooled Copper Dimer. *J. Chem. Phys.* **1986**, *84*, 6560–6566.
- (55) Ho, J.; Polak, M. L.; Ervin, K. M.; Lineberger, W. C. Photoelectron Spectroscopy of Nickel Group Dimers: Ni–2, Pd–2, and Pt–2. *J. Chem. Phys.* **1993**, *99*, 8542–8551.
- (56) Spain, E. M.; Morse, M. D. The 3d8Ni(3F)3d10Cus2s*1 Manifold of Exited Electronic States of NiCu. *J. Chem. Phys.* **1992**, *97*, 4633–4640.
- (57) Fu, Z.; Morse, M. D. Spectroscopy and Electronic Structure of Jet-Cooled NiCu. *J. Chem. Phys.* **1989**, *90*, 3417–3426.
- (58) Balbuena, P. B.; Derosa, P. A.; Seminario, J. M. Density Functional Theory Study of Copper Clusters. *J. Phys. Chem. B* **1999**, *103*, 2830–2840.
- (59) Triguero, L.; Wahlgren, U.; Boussard, P.; Siegbahn, P. Calculations of Hydrogen Chemisorption Energies on Optimized Copper Clusters. *Chem. Phys. Lett.* **1995**, *237*, 550–559.
- (60) Nygren, M. A.; Siegbahn, P. E. M.; Wahlgren, U.; Akeby, H. Theoretical Ionization Energies and Geometries for Nin ($4 < n < 9$). *J. Phys. Chem.* **1992**, *96*, 3633–3640.
- (61) Lide, D. R., Ed.; *Handbook of Chemistry and Physics*; CRC Press: Boca Raton, FL, 1997.
- (62) Ram, R. S.; Bernath, P. F.; Brault, J. W. Fourier Transform Emission Spectroscopy: The Vibration–Rotation Spectrum of CuH. *J. Mol. Spectrosc.* **1985**, *113*, 269–274.
- (63) Marian, C. M.; Blomberg, M. R. A.; Siegbahn, P. E. M. Multireference and Relativistic effects in NiH. *J. Chem. Phys.* **1989**, *91*, 3589–3595.
- (64) Gray, J. A.; Li, M.; Nelis, T.; Field, R. W. The Electronic Structure of NiH: The {Ni+ 3d9 2D} Supermultiplet. *J. Chem. Phys.* **1991**, *95*, 7164–7178.
- (65) Gray, J. A.; Rice, S. F.; Field, R. W. The Electric dipole moment of NiH X2 D5/2 and B2 D5/2. *J. Chem. Phys.* **1985**, *82*, 4717–4718.
- (66) Morse, M. D. Clusters of Transition-Metal Atoms. *Chem. Rev.* **1986**, *86*, 1049.